Power Quality Improvement in Distribution System Using IRP Theory with SMC

Kalagotla Chenchireddy[1]*, V Jegathesan[2]

[1] *Research Scholar, Department of Electrical and Electronics Engineering,*
    Karunya Institute of Technology and Sciences, Coimbatore, 641114, INDIA

[2] *Associate Professor, Department of Electrical and Electronics Engineering,*
    Karunya Institute of Technology and Sciences, Coimbatore, 641114, INDIA

*Corresponding Author: chenchireddy.kalagotla@gmail.com
DOI: https://doi.org/10.30880/ijie.2024.16.02.004

Article Info	Abstract
	This article discusses how to improve power quality in distribution systems by combining (Instantaneous Reactive Power) IPR theory with (Sliding Mode Control) SMC. The distribution system has numerous power quality issues. This paper concentrated primarily on source-side current harmonics. The primary goal of this paper is to reduce source-side current harmonics while also balancing DC-link capacitor voltage. The SMC is used to control the d- and q-axis reference currents. The IPR theory is used in distribution to calculate active and reactive power. The SMC based on IPR theory reduced source current harmonics while maintaining constant DC-link capacitor voltage. The results of MATLAB/Simulation are compared to those of PI and SMC. SMC findings exhibit superior performance than the PI controller.

1. Introduction

Failure of the capacitor bank, increased losses in the electrical equipment and distribution system, noise, vibrations, over-voltage, excessive current owing to resonance, and negative sequence currents in the generator and motor, particularly the rotor, are the main causes of power quality problems. Hearing loss, dielectric breakdown, communication system interference, false metering, and interference with motor controllers and digital controllers are all possibilities. The primary sources of reactive power burden in the distribution system are phase-controlled rectifiers, motors, transformers, and choke inductors. Harmonics in the distribution system cause heating of electrical equipment, damage to equipment, and light flickering. Custom power devices are now used to compensate for harmonics. Filters were once used in distribution to compensate for harmonics. A single-tuned filter was used to eliminate 5th-order harmonics, while a double-tuned filter was used to eliminate 5th and 7th-order harmonics. A second-order higher-damped filter is used to eliminate harmonics of greater than the 11th order. Fractional-order SMC (FO-SMC) compensated for reactive power and eliminated grid harmonics. Positive and negative sequence harmonics were reduced in the wind farm using the FO-SMC single and dual loop control strategies. The super capacitor in this paper was used for DC-link voltage [1]. [2] Used super twisting SMC to compensate for voltage-related power quality issues. The controller responded quickly and was resistant to voltage fluctuations. The controller's response had been verified in various load conditions such as voltage sag, swell, static and dynamic load. The controller works well in a variety of load conditions. D-STATCOM used the input-output feedback linearization method in conjunction with integral SMC.

The reactive power of this paper compensated for no disturbance and internal disturbance conduction. In both no disturbance and internal disturbance conditions, the negative sequence current is compensated [3]. The authors of [4] presented D-STACOM based on FO-SMC. The performance of the proposed controller was evaluated

under various conditions such as voltage sag, swell, and load imbalanced and balanced situations. The FO-SMC had a very fast response time, high accuracy, robustness, and a low THD value. The authors of [5] proposed a nonlinear controller based on SMC for closed-loop operation of the three-phase MLI with a reduced switch count. The simulation results in this paper are validated under active and reactive power step-change conditions. The proposed controller successfully changed the grid frequency and load change time. SMC based on space vector modulation (SVM) was implemented for a grid-connected 3L-NPC inverter [6]. The source-side current harmonics were reduced by the proposed controller. The results meet the IEEE-519 international standard. Low THD grid currents, less switching loss, a high-power factor, and dependable operation are just a few benefits of the SVM-based SMC. The FO-SMC implemented for controlling D-STATCOM is referenced in [7]. During a fault condition, the proposed controller had a fast response, high robustness, and high accuracy. Reduced switch count grid connected MLI was implemented in [8]. SMC was in charge of the proposed topology. Results from the PI controller and the SMC were contrasted. Improved power quality distribution was achieved by installing the SMC of the static shunt compensator [9]. The authors of [10] compared a range of voltage balancing super capacitor circuits.

2. D-STATCOM Model Circuit

The primary goals of D-STACOM are reactive power compensation and harmonic elimination; it will maintain voltage regulation and balance unbalanced load currents. The primary goals of this paper are to reduce source-side current harmonics while maintaining constant DC-link voltage. Figure 1 depicts a D-STACOM circuit with three voltage source inverters. The supply-side voltages are Vsa, Vsb, and Vsc. The source side currents are Isa, Isb, and Isc. The three-phase load currents are ILa, ILb, and ILc. As a D-STACOM circuit, a three-phase two-leg inverter is used. This paper used a D-STACOM circuit controlled by an IPR-based SMC controller. Only a reactive power ideal case is drawn by the D-STACOM. In practice, there is some switching loss in the D-STATCOM circuit; these losses are typically real power losses. There is no need to connect the D-STATCOM circuit to a DC source; a small energy-storing capacitor suffices. If the removed load in the circuit, it looks like an active rectifier circuit in fig.1. In this case, the capacitor voltage must equal the source voltage's peak. The capacitor voltage in the D-STATCOM circuit must be at a peak of 1.6 to 2 times. Compensation is not possible if the capacitor voltage is less than 1.6 times.
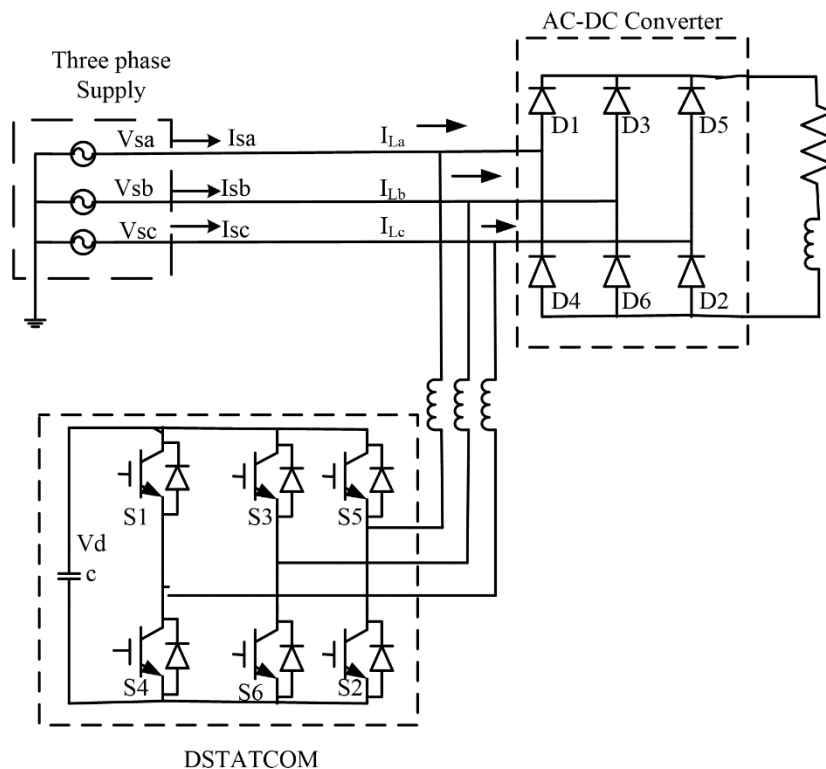
Fig. 1 *D-STATCOM model circuit*

2.1 DC Voltage Regulation

The capacitor voltages should be consistent if there is no loss in the D-STACOM circuit. However, in a real-world scenario, the PWM functioning of the D-semiconductor STATCOM's switches results in some switching losses.

Energy is delivered to the capacitor on the DC-link. [11]- [13] A little amount of average actual power must be consumed to keep the dc-link voltage steady. By incorporating dc voltage regulation into the control technique, this may be demonstrated.

Mathematical analysis of a P-Q theory:

$$P_{g_i} = v_{dg_i} i_{dg_i} + v_{qg_i} i_{qg_i} \text{ and } Q = v_{qg_i} i_{dg_i} - v_{dg_i} i_{qg_i} \tag{1}$$

Equation (1) represents active and reactive powers.

$$i_{dref} = \frac{v_{qg} Q_{ref} + v_{dg} P_{ref}}{v_{dg}^2 + v_{qg}^2} \text{ and } i_{qref} = \frac{v_{qg} P_{ref} - v_{dg} Q_{ref}}{v_{dg}^2 + v_{qg}^2} \tag{2}$$

Equation (2) represents direct axis and quadrature axis currents, which are represented by Idref and Iqref.

$$v dinv_d - R_f i_{dg} - L_f \frac{di_{dg}}{dt} + \omega L_f i_{qg} - v_{dg} = 0 \tag{3}$$

$$v qinv_d - R_f i_{qg} - L_f \frac{di_{qg}}{dt} + \omega L_f i_{dg} - v_{qg} = 0 \tag{4}$$

$$\frac{dx}{dt} = f(x) + g(x)u \tag{5}$$

Equation (5) represents the second-order differential equation, g(x) means the non-linear function, and u means control input.

$$f(x) = \begin{bmatrix} -\dfrac{R_f}{L_f} i_{dg} + \dfrac{X_f}{L_f} i_{qg} - \dfrac{1}{L_f} v_{dg} \\[2ex] \dfrac{R_f}{L_f} i_{qg} + \dfrac{X_f}{L_f} i_{dg} - \dfrac{1}{L_f} v_{qg} \end{bmatrix} \tag{6}$$

$$g(x) = \begin{bmatrix} \dfrac{1}{L_f} & 0 \\[2ex] 0 & \dfrac{1}{L_f} \end{bmatrix} x = \begin{bmatrix} i_d \\ i_q \end{bmatrix} u = \begin{bmatrix} v_{dinv} \\ v_{qinv} \end{bmatrix}$$

$$\lambda = A(x) + B(x)U \tag{7}$$

$$U = (-B^{-1}(x) * A(x)) + (B^{-1}(x) * \lambda) \text{ or } \quad U = \alpha(x) + \beta(x)\lambda \tag{8}$$

$$\alpha(x) = -B^{-1}(x) * A(x) \text{ and } \beta(x) = B^{-1}(x)$$

$$B(x) = \begin{bmatrix} g_{11}(x) & 0 \\ 0 & g_{22}(x) \end{bmatrix} A(x) = \begin{bmatrix} f_{11}(x) \\ f_{21}(x) \end{bmatrix}$$

$$\lambda = \begin{bmatrix} \lambda_{11} & \lambda_{12} \end{bmatrix}^T = \begin{bmatrix} \dfrac{di dg}{dt} & \dfrac{di qg}{dt} \end{bmatrix}^T \tag{9}$$

$$Y = \begin{bmatrix} i dg & i qg \end{bmatrix}^T \tag{10}$$

I_{dg} and I_{qg} are the DQ-reference frame currents. V_{dg} and Vdg are the DQ-reference frame voltages. I_{dref} and I_{qref} are the reference D and Q-axis currents. I_{dg} and I_{qg} are the actual currents. The comparator compared reference current and actual current, comparator output connected to the PI controller. PI controller converts DQ-axis currents to DQ-axis voltages. Inverse Clarke transformation it converts V_{dref} and V_{qref} to V_{aref}, V_{bref} and V_{cref}. Inverse Clarke transformation is used for converting two-phase to three-phase.
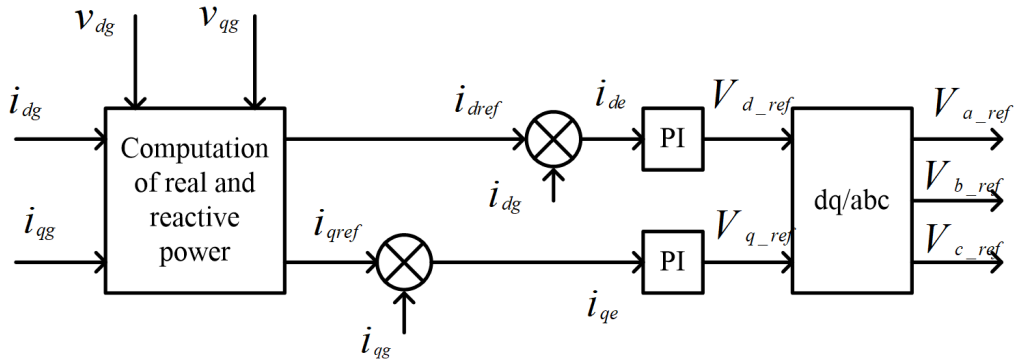
Fig. 2 *IPR theory with PI controller*

3. Sliding Mode Control

The D-STACOM circuit is classified into mainly two types, one is CSI-fed D-STATCOM and the other is VSI-fed D-STACOM. The CSI-fed D-STATCOM has some disadvantages, these are more weight, more cost and it occupies more space. The VSI-fed D-STATCOM occupies less space and stores energy easily in an electrolyte capacitor. Fig.3 shows the VSI-fed D-STATCOM schematic diagram in this circuit, the load current block is used for measuring load side current. The source voltage block is used for measuring source side voltages. The D-STATCOM block is used for measuring compensating currents. The DC link voltage of the capacitor block is used for measuring the DC – link voltage. The pulse generator block converts Reference signals to PWM pulses. Three-phase VSI is used for D-STACOM.
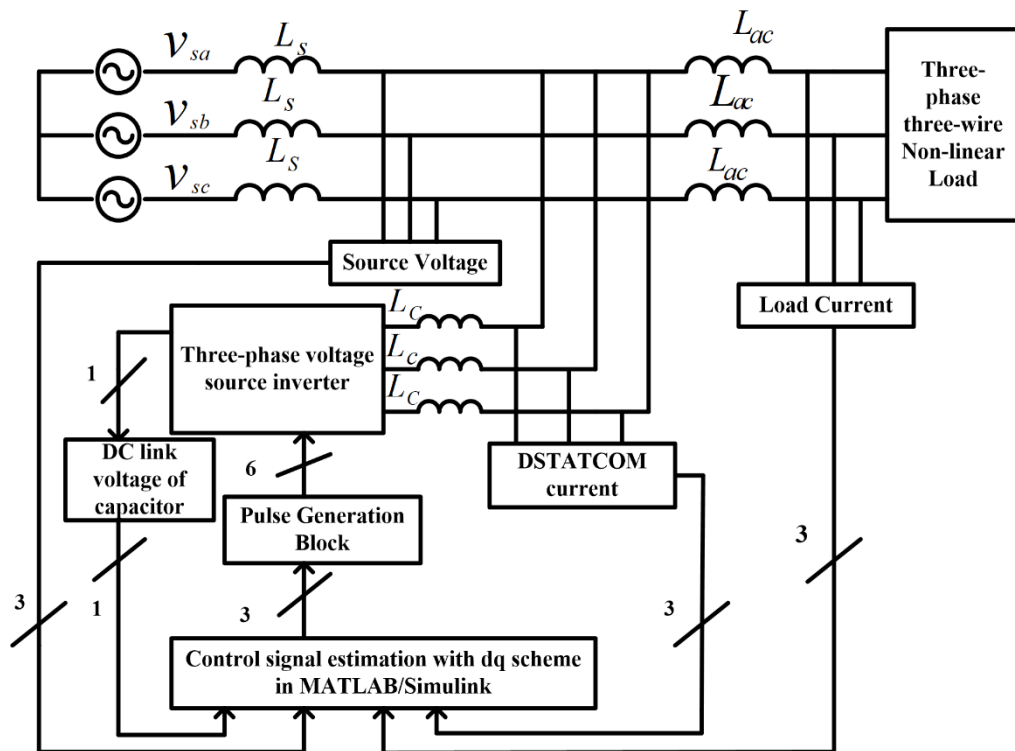
Fig. 3 *D-STATCOM schematic diagram*

A control D-STATCOM's algorithm is shown in Fig. 4. The voltages Vdc1 and Vref are the actual and reference DC-link voltages. The voltages are given to a PI controller. The output of the PI controller is power loss in switching devices. [14]- [15] This amount of power loss is occurring in switching devices. This total control scheme deals with power form, the losses are also calculated with power form. iLa, iLb, and iLc are the load currents, these currents convert from three-phase to two-phase i-alpha and i-beta use Clark transformation. V-alpha and V-beta are the d-axis and q-axis voltages. These voltages are converted from three-phase supply voltages to DC quantities. Instantaneous power calculation block converts from dc voltages and currents to P and Q powers.
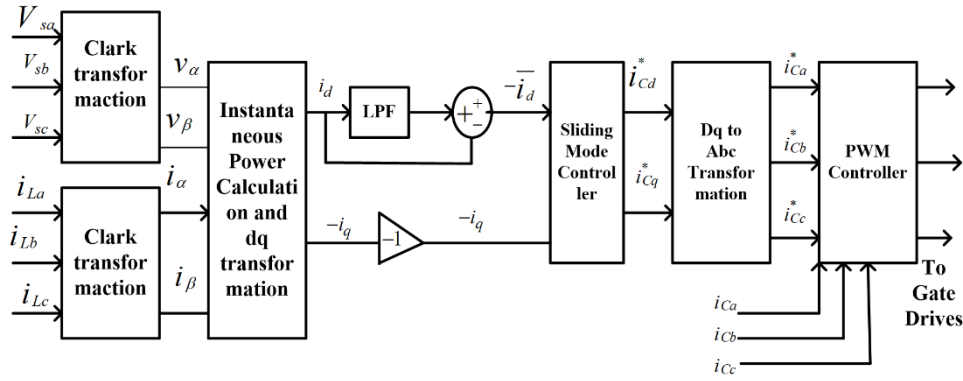
Fig. 4 *D-STATCOM control scheme*

Fig. 5 shows IPR theory with SMC. The SMC is one of the most popular control systems in nonlinear load

$$U(t) = U_{eq}(t) + U_{sw} = U_{eq}(t) + \rho.\tanh(\sigma) \tag{11}$$

The equation represents the comparable control law and switching law that make up the SMC (11). Where the sliding is surface and is a positive constant.

$$\sigma(t) = \frac{der(t)}{dt} + K_t er(t) \tag{12}$$

The sliding surface matrix σ with $\sigma_1 = i_{dg} - i_{dref}$ and $\sigma_2 = i_{qg} - i_{qref}$ as elements can be represented as

$$\sigma = \begin{bmatrix} \sigma_1 & \sigma_2 \end{bmatrix} \tag{13}$$

The Lyapunov function can be represent as $G = \frac{1}{2}\sigma^2$ (14)

$$\frac{dG}{dt} = \sigma\dot{\sigma}^T < 0 \tag{15}$$

$$\dot{\sigma}_1 = -\rho_1.\tanh(\sigma_1) \text{ and } \dot{\sigma}_2 = -\rho_2.\tanh(\sigma_2) \tag{16}$$

$$\dot{\sigma}_1 = -\rho_1.\tanh(i_{dg} - i_{dref}) \text{ and } \dot{\sigma}_2 = -\rho_2.\tanh(i_{qg} - i_{qref}) \tag{17}$$

With the obtained new dynamics using SMC, the state vector can be represented as

$$\lambda_1 = \begin{bmatrix} \lambda_{11} \\ \lambda_{12} \end{bmatrix} = \begin{bmatrix} -\rho_1.\tanh(i_{dg} - i_{dref}) \\ -\rho_2.\tanh(i_{qg} - i_{qref}) \end{bmatrix} \tag{18}$$

I$_{dref}$ and I$_{qref}$ is attainable from (2). If the device's parameter changes, the matrix for the device will alternate between the two sides, and the device may then be represented as

$$\dot{X} = (A + \Delta A)X + B(U_{eq} + U_{sw}) \tag{19}$$

$$\dot{X} = (A + BU_{eq} + \Delta AX + + B\rho\tanh(\sigma) \tag{20}$$

$$B\rho > \Delta AX \text{ or } \rho > \begin{bmatrix} B^{-1}\Delta AX \end{bmatrix} \tag{21}$$

As aforesaid, ρ is an appositive constant; however, to cancel out the mistakes on account of parameter variations, running factor changes, and outside disturbances, ρ have to be large.
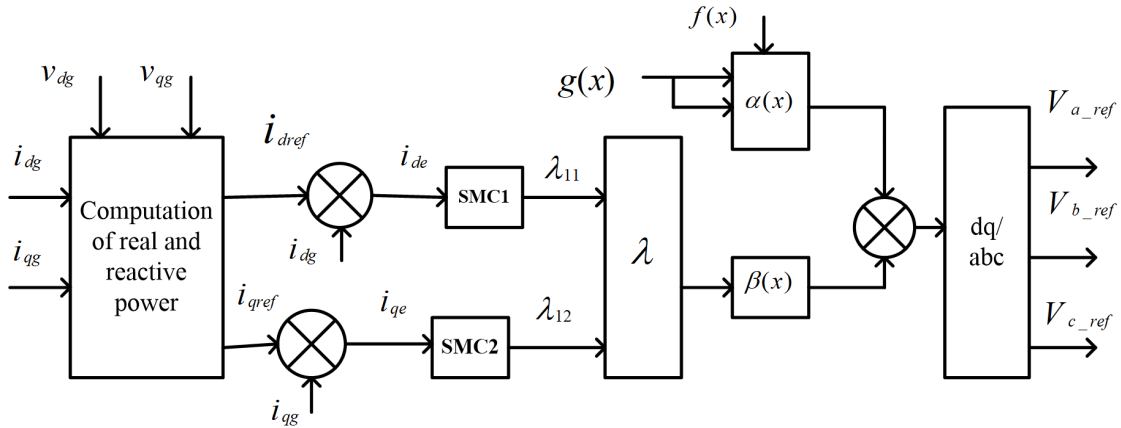
Fig. 5 *IPR theory with SMC*

Table 1 *Comparison table*

Control algorithm	Outcome
FO-SMC [1]	Power quality had improved in grid and wind farm integrated circuits. The controller effectively eliminated the oscillations of the active and reactive power. The DFIG stator current harmonics are reduced.
Super twisting SMC [2]	The control algorithm eliminated voltage-related power quality problems. The controller responded very fast and provided robustness to voltage disturbance.
Integral SMC [3]	The input-output feedback linearization method along with integral SMC had applied to D-STATCOM. The reactive power had compensated in no disturbance and internal disturbance conduction. The negative sequence current is also compensated in no disturbance and internal disturbance condition
FO-SMC [4]	The proposed controller simulation results are compared with the PI controller. The FO-SMC had a very high response time, accuracy, and robustness. The THD value of the FO-SMC controller is 0.52% during voltage sag/swell conditions.
SMC [5]	• In this paper, a nonlinear controller for closed-loop operation of a three-phase MLI with a reduced switch count is presented. The simulation results are verified during active and reactive power step-change conditions. The proposed controller had a well-operated change in grid frequency and load change time.
SVM-based SMC [6]	This paper presents the sliding mode current controller implemented. The controller-maintained grid current international standards IEC6000-1-2-2 and IEEE 555.
Proposed SMC	The Proposed SMC has maintained grid currents IEEE 519 Standard. The grid side current THD is 2.76% The DC-link capacitor voltage is maintained constant.

4. Simulation Results

4.1 IPR Theory with PI Controller

Fig.6 shows four waveforms A-phase supply voltage, supply current, compensating current, and load current. The magnitude of the input supply voltage is 230V. The input current Is low in the first cycle 0 to 0.02 sec. the reaming cycles maintained a constant current 50A. The field current I_f generated by the D-STACOM circuit. The current I_L is connected bridge rectifier input. The THD waveform of the grid side A-Phase supply current is shown in Fig. 7. The A-phase THD value is 5.65%.
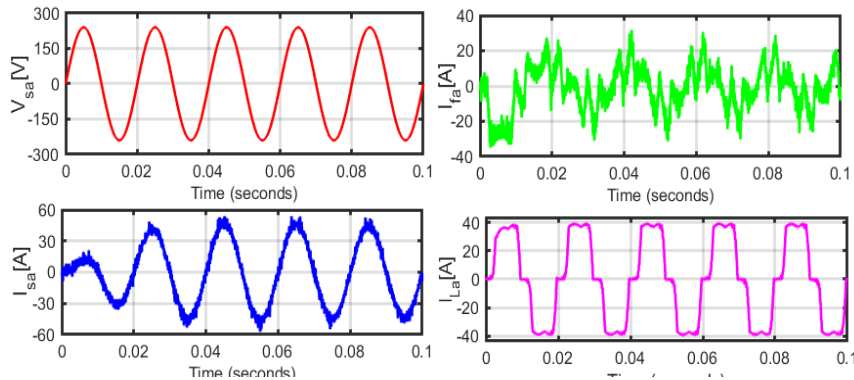
Fig. 6 *Simulation results in A-phase with PI controller*
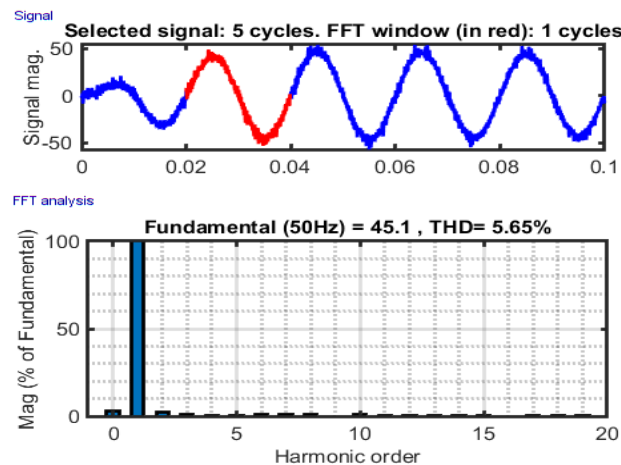
Fig. 7 *Harmonic spectrum of A-phase current of the grid supply with PI*

4.2 IPR Theory with SMC Controller

This section presents DSTATCOM with SMC results. The SMC controller mainly selected for controlling uncertainties and nonlinearity. The SMC is a combination of equivalent control law and switching law. The equivalent control law controlling parameters of system and switching it reduces chattering phenomenon of the system. Before connecting DSTATCOM source current is follows the load current. Fig.8 shows simulation results in A-phase with SMC. The simulation results are A-phase both PI and SMC nearly the same, but the harmonic content is different and settling time of sine wave also same. Fig.9 shows three-phase supply voltage, supply current, compensation current, and load current. The three-phase supply voltage is having 230V magnitude and 120^0 phase shift. The three-phase supply current takes 0 to 0.02 sec. time for settling constant current, after 0.02 sec the supply current waveform is maintained constant current 50A. The D-STATCOM current is represented by compensation current for the supply side. The 3-phase load current is a diode bridge rectifier input current. This current is not in the sinusoidal waveform. The main functions of SMC are it brings system from trajectory to equilibrium. Sliding surface is it reduces chattering and it brings zero error in current.

Three alternatives single-phase current waveforms and the voltage across the DC-link capacitor are shown in Fig. 10. The source current is represented by Is, the magnitude of source current 40A, this current undershoots 0

to 0.02sec after 0.02 sec the waveform maintained constant current. The D-STATCOM current is represented by If, this current is used for compensation. The load current is represented by IL; this current is maintained constant magnitude from starting position. The DC-link capacitor voltage is represented by Vdc, this voltage decreased from 0 to 0.02sec, the voltage increased from 0.02 sec to 0.1 sec, and after 0.1 sec the voltage maintained a constant magnitude. The relationship between the source current and the DC-link capacitor voltage is kept linear. The DC-Link capacitor rating is high in DSTATCOM, in case diode bridge rectifier removed the DSTATCOM acts as converter and DC-link capacitor acts as Load. The converter output voltage is more than AC supply voltage and current. This reason this paper used as high DC-link capacitor. Fig.11 shows that A-Phase source current waveforms are PI and SMC, the PI and SMC results are almost the same with a small THD difference. The source current's THD waveform with the SMC controller is shown in Fig. 12. The source current's THD value is 2.76%. The comparative study of the DSTATCOM control with PI/SMC is shown in fig.11. The Table .2 shows the comparative performance of DSTATCOM with PI/SMC. The settling times for both PI as well as SMC same. The value of total harmonics distortion (THD) of source current with PI controller is 5.65%. After compensation SMC with DSTATCOM, the THD of source current is reduced to 2.76%. The value of THD recorded immediately after settling sine waveform.
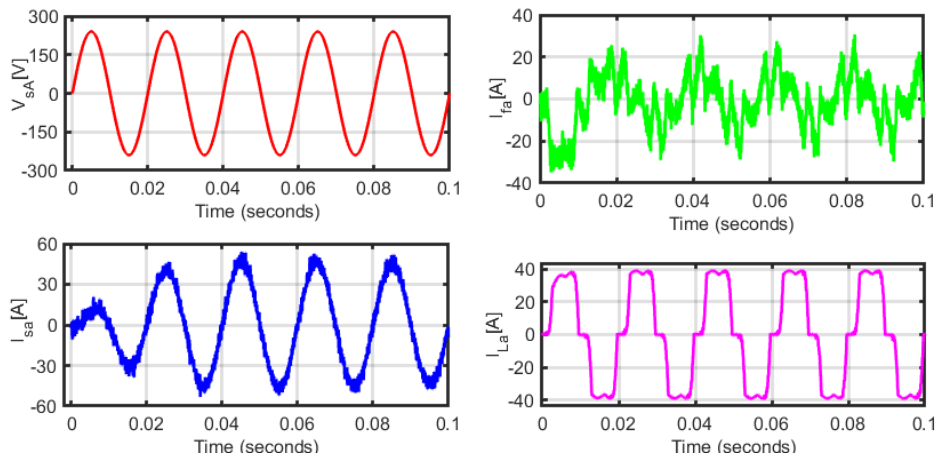
Fig. 8 *Simulation results in A-phase with SMC*
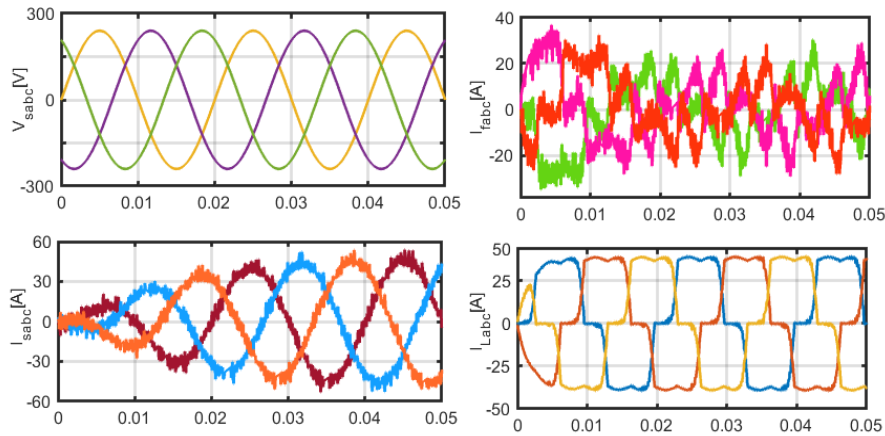
Fig. 9 *Simulation results in three-phase with SMC controller*
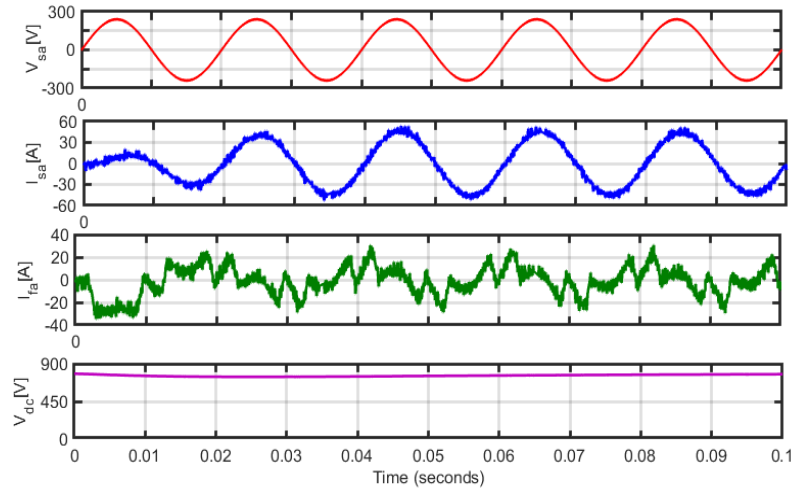
Fig. 10 *Shows A-phase supply, D-STATCOM and load current waveforms as well as DC capacitor voltage*

5. Conclusion

This study examines how IRP theory and SMC can improve power quality in distribution systems. The main outcomes of this paper are reducing supply current side harmonics and maintaining constant voltage in the DC-link capacitor. The three-phase two-level inverter acts as a D-STATCOM circuit in this paper. The IRP theory is used for calculating Real and Reactive power. The SMC is mainly used for controlling non-linear systems. In this paper, SMC results are compared with the PI controller. The performance of SMC is very fast response, high accuracy, and very high robustness, with the lowest THD of 2.76% and steady-state time of 0.03 sec. the overall performance of SMC is good.
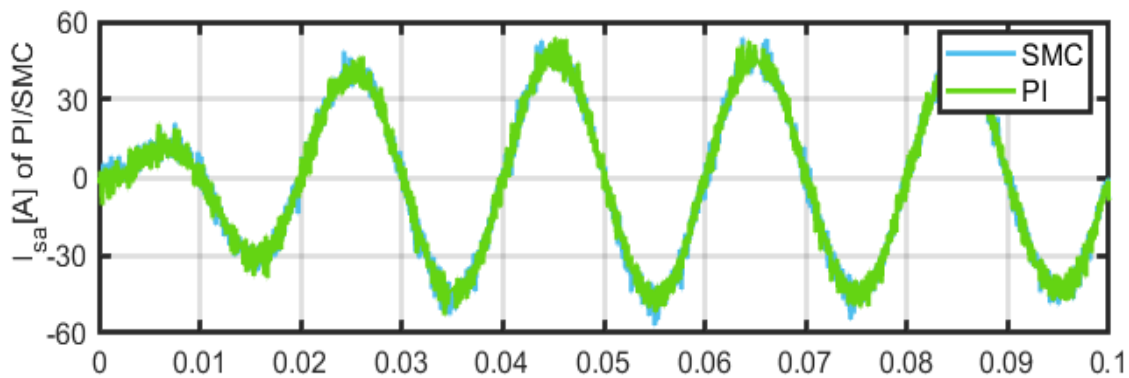
Fig. 11 *The A-phase supply current comparison wave from*
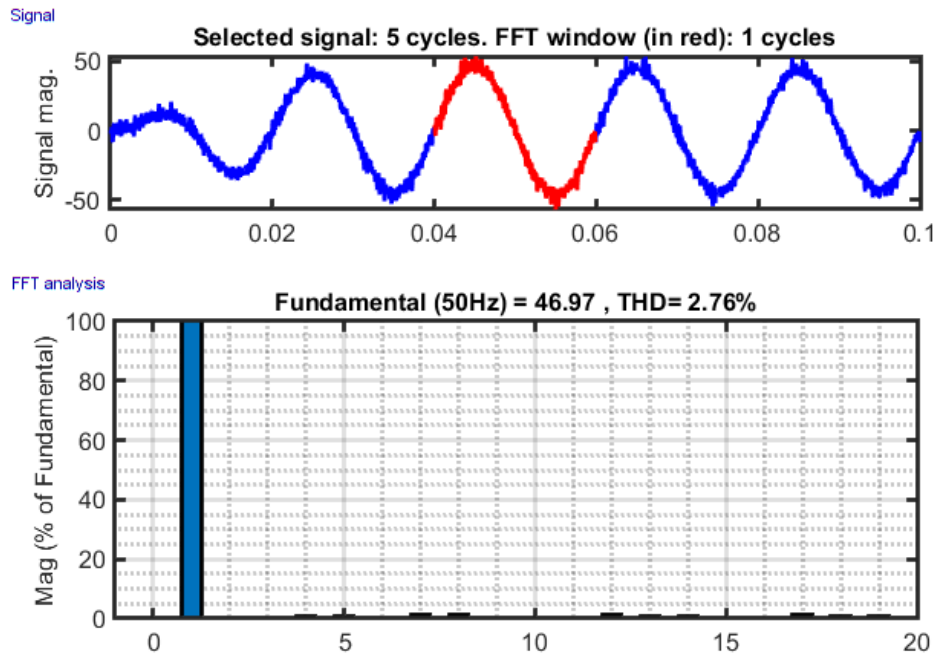
Fig. 12 *Harmonic spectrum of phase current of the grid supply with SMC*

Table 2 *Comparative study of DSTATCOM with PI/SMC*

Parameter	DSTATCOM with PI	DSTATCOM with SMC
Source Current THD	5.65 %	2.76 %
Settling Time (Source Current)	1-2 cycles	1-2 cycles

Acknowledgement

Conflict of Interest

Authors declare that there is no conflict of interests regarding the publication of the paper.

References

[1]   Kerrouche, K. D. E., Wang, L., Mezouar, A., Boumediene, L., & Van Den Bossche, A. (2019). Fractional-order sliding mode control for D-STATCOM connected wind farm based DFIG under voltage unbalanced. Arabian Journal for Science and Engineering, 44(3), 2265-2280.
[2]   Ullah, M. F., & Hanif, A. (2021). Power quality improvement in distribution system using distribution static compensator with super twisting sliding mode control. International Transactions on Electrical Energy Systems, 31(9), e12997.
[3]   Xia, M., & Mao, Y. (2013). Integral sliding mode control strategy of D-STATCOM for unbalanced load compensation under various disturbances. Mathematical Problems in Engineering, 2013.
[4]   Ahmed, T., Waqar, A., Elavarasan, R. M., Imtiaz, J., Premkumar, M., & Subramaniam, U. (2021). Analysis of fractional order sliding mode control in a d-statcom integrated power distribution system. IEEE Access, 9, 70337-70352.
[5]   Gowd, G. E., Sekhar, P. C., & Sreenivasarao, D. (2018). Real-time validation of a sliding mode controller for closed-loop operation of reduced switch count multilevel inverters. IEEE Systems Journal, 13(1), 1042-1051.
[6]   Sebaaly, F., Vahedi, H., Kanaan, H. Y., Moubayed, N., & Al-Haddad, K. (2016). Design and implementation of space vector modulation-based sliding mode control for grid-connected 3L-NPC inverter. IEEE Transactions on Industrial Electronics, 63(12), 7854-7863.

[7]   Ahmed, T., Waqar, A., Al-Ammar, E. A., Ko, W., Kim, Y., Aamir, M., & Habib, H. U. R. (2020). Energy management of a battery storage and D-STATCOM integrated power system using the fractional order sliding mode control. CSEE Journal of Power and Energy Systems, 7(5), 996-1010.

[8]   Gowd, G. E., Sreenivasarao, D., & Vemuganti, H. P. (2021). Sliding mode controller for extraction and supply of photovoltaic power using switched series parallel sources reduced switch count multilevel inverter. IET Power Electronics, 14(4), 834-850.

[9]   Singh, B., Sekhar, V. C., & Kant, K. (2014). Sliding mode control of static shunt compensator. In 2014 IEEE International Conference on Power Electronics, Drives and Energy Systems (PEDES) (pp. 1-7)

[10] Bt, P. S., Phaneendra, B. B., & Suresh, K. (2019). Extensive review on Super capacitor cell voltage balancing. In E3S Web of Conferences (Vol. 87, p. 01010)

[11] Heidari, M. A., Nafar, M., & Niknam, T. (2022). A Novel Sliding Mode Based UPQC Controller for Power Quality Improvement in Micro-Grids. Journal of Electrical Engineering & Technology, 17(1), 167-177.

[12] Huang, S., Wang, J., Huang, C., Zhou, L., Xiong, L., Liu, J., & Li, P. (2022). A fixed-time fractional-order sliding mode control strategy for power quality enhancement of PMSG wind turbine. International Journal of Electrical Power & Energy Systems, 134, 107354.

[13] Mousavi, Y., Bevan, G., Kucukdemiral, I. B., & Fekih, A. (2022). Sliding mode control of wind energy conversion systems: Trends and applications. Renewable and Sustainable Energy Reviews, 167, 112734.

[14] Ramos-Paz, S., Ornelas-Tellez, F., & Rico-Melgoza, J. J. (2022). Power quality enhancement through ancillary services provided by power electronic converters. Electric Power Systems Research, 209, 107934.

[15] Chenchireddy, K., & Jegathesan, V. (2022). Three-Leg Voltage Source Converter-Based D-STATCOM for Power Quality Improvement in Electrical Vehicle Charging Station. In AI Enabled IoT for Electrification and Connected Transportation, pp. 235-250